J. Fluid Mech. (1992), *vol.* 238, *pp.* 31–54
Printed in Great Britain

Three-dimensional vortex formation from an oscillating, non-uniform cylinder

By F. NUZZI, C. MAGNESS AND D. ROCKWELL
Department of Mechanical Engineering and Mechanics, 354 Packard Laboratory 19, Lehigh University, Bethlehem, PA 18015, USA

(Received 21 March 1991 and in revised form 14 September 1991)

A cylinder having mild variations in diameter along its span is subjected to controlled excitation at frequencies above and below the inherent shedding frequency from the corresponding two-dimensional cylinder. The response of the near wake is characterized in terms of timeline visualization and velocity traces, spectra, and phase plane representations. It is possible to generate several types of vortex formation, depending upon the excitation frequency. Globally locked-in, three-dimensional vortex formation can occur along the entire span of the flow. Regions of locally locked-in and period-doubled vortex formation can exist along different portions of the span provided the excitation frequency is properly tuned. Unlike the classical subharmonic instability in free shear flows, the occurrence of period-doubled vortex formation does not involve vortex coalescence; instead, the flow structure alternates between two different states.

1. Introduction

In recent years there have been a number of important theoretical advances describing the absolute instabilities of shear flows, including the generic case of a bluff-body wake. Huerre & Monkewitz (1985), Koch (1985), Monkewitz & Nguyen (1987), Triantafyllou, Triantafyllou & Chryssostomodis (1986), and Monkewitz (1988) put forth their own theoretical advances and assess related studies of absolute instabilities. The concept of a global instability, as opposed to an absolute instability, is defined by Chomaz, Huerre & Redekopp (1988). Their studies showed that in order for globally-unstable oscillations of a shear flow to occur, not only must the flow be absolutely unstable, but the region of instability must attain a sufficiently large size. An important consequence of the global instability of a bluff-body wake is the generation of a highly coherent and nonlinear oscillation, in the absence of external excitation. Therefore, perturbation of this global instability, at a frequency other than its self-excited one, can give rise to a number of interesting phenomena. The variety of locked-in and quasi-periodic status of response attainable by forced excitation of a cylinder are addressed by Williamson & Roshko (1988) and Ongoren & Rockwell (1988*a*, *b*). The onset of spectral broadening and the production of a large number of spectral components in the near-wake owing to instabilities from a stationary cylinder, from external excitation of a two-dimensional rigid cylinder, or from a cylinder undergoing aeroelastic oscillations in one of its spanwise modes is described by Sreenivasan (1985), Van Atta & Gharib (1987), Olinger & Sreenivasan (1988), Karniadakis & Triantafyllou (1989*a*, *b*), and Karniadakis & Triantafyllou (1990) who interpret the wake response using concepts of chaos.

The onset of chaos in a closed fluid system, in particular the Rayleigh–Bénard

instability, has been extensively investigated in recent years. The forcing function for this type of instability is the temperature difference ΔT across the horizonatal layer of fluid. Gollub & Benson (1980) define the several possible routes to turbulence in this free-convection problem. These routes include: quasi-periodicity and phase-locking; subharmonic (period-doubling) bifurcations; occurrence of three distinct frequencies; and intermittent noise. The route involving successive period-doubling is discussed in further detail by Gollub, Benson & Steinman (1980). In their investigation, they point out the difficulty of determining whether the occurrence of non-periodicity was preceded by more than two successive period doublings. Small variations in the system parameters, e.g. geometry, Prandtl number, could generate a second incommensurate frequency after one period doubling. In other words, 'pure' period doubling beyond the first was difficult to achieve. Giglio, Musazzi & Perini (1981) emphasize the importance of the initial state of the Rayleigh–Bénard system. By applying a very large temperature difference across the horizontal fluid layer, then a succession of small temperature differences, the system could be driven to well-defined dynamical states, with period-doubled bifurcations up to $f_1/16$, in which f_1 is the fundamental instability frequency. A theoretical framework for describing the successive period-doubled bifurcations of nonlinear systems is given by Feigenbaum (1980). His prediction of the amplitudes of the spectral peaks arising from the period-doublings is in accord with the first two bifurcations observed experimentally by Gollub *et al.* (1980).

These well-documented investigations of period-doubling in a closed fluid system raise the issue of whether an equivalent phenomenon can occur in an open fluid system. Karniadakis & Triantafyllou (1990, 1992) have demonstrated numerically the occurrence of period-doubling in the secondary instability from a circular, stationary cylinder at low Reynolds number. Three-dimensionality of the flow structure is a necessary ingredient of this period-doubling process. In the present investigation, the focus is on inducement of period-doubled vortex formation from a non-uniform cylinder subjected to forced excitation. It is intended that 'detuning' of the highly coherent vortex formation in the spanwise direction, arising from the gradual variation of the cylinder diameter, will promote the occurrence of non-periodic and period-doubled states. Indeed, the preliminary studies of Rockwell, Nuzzi & Magness (1990, 1991) suggest that this approach can lead to an effective and repetitive destabilization of the near-wake vortex formation.

Quite apart from these considerations of chaotic response, the development of three-dimensional flow structure from stationary trailing-edges has received considerable attention in recent years. Meiburg & Lasheras (1988) and Lasheras & Meiburg (1990) review the three-dimensional structure of wakes and describe the symmetry characteristics of the three-dimensional vorticity configurations in wakes. Employing combined experimental and numerical approaches, Lasheras & Meiburg (1988) examined the evolution of the wake from the trailing-edge of a thin flat plate having spanwise perturbations. As a consequence of the induction of vorticity from either side of the trailing-edge of the plate, there are 'braids' that connect neighbouring large-scale (Kármán) vortices taking the form of counter-rotating pairs of streamwise vortices. In their subsequent work, Lasheras & Meiburg (1990) relate the three-dimensional vorticity modes to the initial conditions. The effects of both fundamental and subharmonic perturbations are addressed. An important feature of the three-dimensional structure is the induction of spanwise undulations of the large-scale (Kármán) vortices; such undulations can exhibit either an in-phase or varicose pattern.

Taking into account the absolute (or global) instabilities of bluff-body wake flows, in particular the flow past a cylinder, Triantafyllou (1990) describes, using concepts of linear stability, the mechanisms giving rise to three-dimensional patterns in two-dimensional flows. The first class of instability is characterized by steady modulations of the average two-dimensional flow, which gives rise to three-dimensional modulations of the instability; this type of instability is basically the secondary instability. The second class involves the generation of three-dimensional wave patterns from a three-dimensional non-uniformity, for example, spanwise variations in cylinder diameter. It is possible to produce organized, three-dimensional patterns in the downstream wake by means of linear resonances.

As described in the foregoing, the concepts of lock-in and quasi-periodic response of the wake from a two-dimensional cylinder subjected to controlled excitation are well recognized. The nature of forced, three-dimensional flow structure along the span of the wake and its interpretation in terms of locked-in and quasi-periodic (low-order chaotic) response deserves attention. In particular, the issue arises as to whether it is possible to induce coexisting and repeatable modes of different classes of vortex formation along the span of the wake. We presume that three-dimensionality of the wake structure will be inherent to the possible modes such as lock-in, and simple and complex subharmonic modulation of the vortex formation, and therefore gently guide the three-dimensional development of the near-wake vortices from a cylinder having gradual spanwise variations. This three-dimensional segment of the cylinder is bounded by long, two-dimensional segments on either side of it in order to allow the three-dimensional flow structure to develop within a well-defined two-dimensional wake.

2. Experimental system and techniques

The overall objective of this experiment is to determine the modes of vortex formation from a cylinder having very gradual spanwise non-uniformity when subjected to controlled oscillations. The spanwise variation of the cylinder diameter is illustrated in figure 1. The total length L of the cylinder, relative to its nominal diameter D was $L/D = 85$. The spanwise extent of the cylinder non-uniformity was $6D$, centred at the midspan. The radii of curvature of the concave and convex regions of the non-uniformity were $45D$ and $23D$, respectively. This configuration having very gradual non-uniformity was arrived at after considering several cylinder geometries. It generated three-dimensional patterns of vortex formation that gradually evolved under controlled excitation, with minimal concentration of streamwise vorticity in the very near wake. For those geometries characterized by an abrupt change in diameter, the well-defined patters of vortex formation described in this study were not evident.

The flow velocity was maintained at 23.54 mm/s corresponding to a Reynolds number based on the cylinder diameter D of $U_\infty D/\nu = 145$. This value of Reynolds number was based on observations of vortex formation from the corresponding stationary two-dimensional cylinder by Gerrard (1978) and Unal & Rockwell (1988). At $Re = 145$, the magnitude of the negative base pressure is high, corresponding to pronounced and highly coherent vortex formation. Moreover, at this value of Reynolds number, there is an absence of small-scale, spanwise, three-dimensionality of the flow structure. Based on the observations of Gerrard (1978), when a Reynolds number $Re = 200$ is attained, these small-scale structures complicate the formation of the primary vortices shed from the stationary cylinder. Of course, oscillation of the

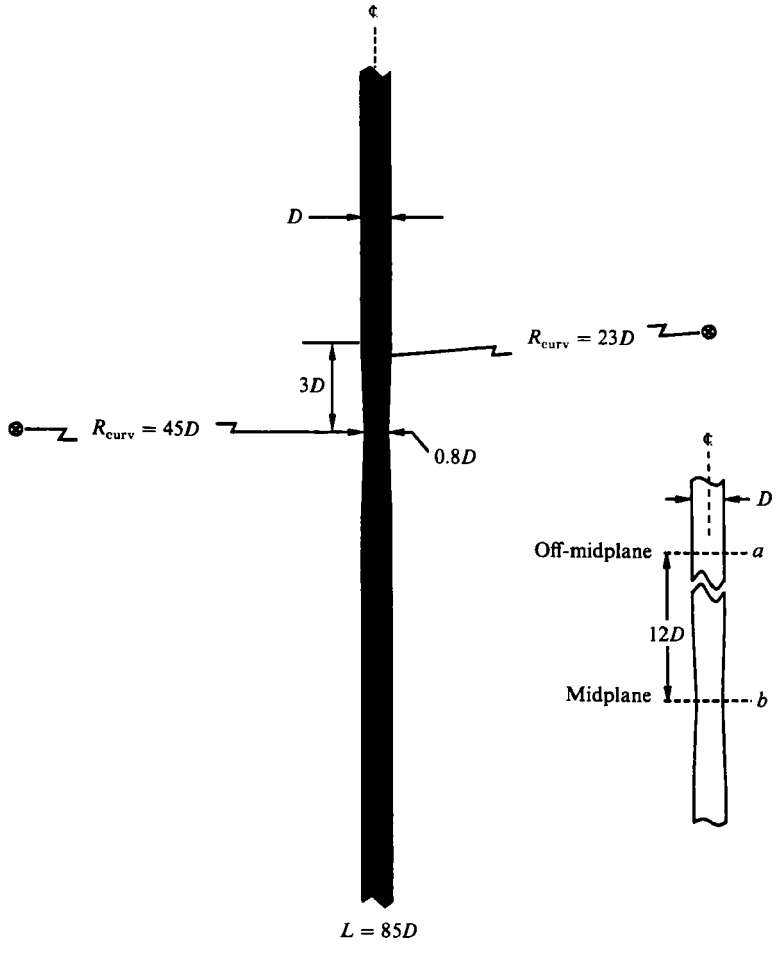

FIGURE 1. Schematic illustrating geometry of cylinder having gradual spanwise variation in diameter. Planes *a* and *b* of flow visualization and velocity measurement are indicated. Plane *b* corresponds to midplane of three-dimensional portion of cylinder and off-midplane *a* represents location within region of two-dimensional vortex formation from cylinder.

cylinder near or at the frequency of inherent vortex formation minimizes the three-dimensionality of the spanwise structure.

The cylinder was mounted on a Daedel traverse table, which was free to move in the cross-stream direction. This table was driven by a Compumotor, which operates on the principle of a controlled stepping motor, but with approximately 10000 steps per revolution, thereby giving an output similar to that of a d.c. servomotor. The cylinder was placed vertically in a free-surface water channel, thereby allowing the entire forcing system and the intermediate connections to be located above the water channel. the cylinder was forced at frequency f_e relative to the inherent vortex formation frequency f_0^* from the two-dimensional portion of the cylinder at rest. In the presence of cylinder oscillation, the natural vortex formation frequency f_0 differed slightly from f_0^*. The amplitude A of oscillation was 2.3 mm, corresponding to $A/D = 0.1875$.

Flow visualization was accomplished with the hydrogen-bubble technique. A 0.025 mm diameter platinum wire was stretched between the ends of either a

horizontal or vertical probe, depending upon the region of interest. For flow visualization in horizontal planes (orthogonal to the cylinder axis) at spanwise locations *a* and *b* in figure 1, the wire was located upstream of the cylinder. The distance between planes *a* and *b*, designated as off-midplane and midplane locations respectively, was suffiently large (12*D*) to ensure that the visualization in plane *a* represented a truly two-dimensional region of the flow structure. For visualization of the spanwise flow structure, the wire was oriented parallel to the axis of the cylinder; it was offset by a distance $0.8 \leqslant y/D \leqslant 2.0$ in the cross-stream direction at a distance $x/D = 6$ downstream of the cylinder axis. In order to generate timelines having small pulse duration, a custom-designed, high-power bubble generator was employed. Digital control of the pulse duration and spacing allowed generation of extremely fine timelines, allowing definition of the flow structure beyond that attainable with a classical hydrogen-bubble generator.

Bubble generation in the horizontal plane was illuminated with a Videologic stroboscopic light, and images were recorded on the Videologic Instar IV system at a rate of 120 frames per second. Supplementary illumination was achieved with a 120 W Bogen studio light oriented at different angles with respect to the test section. For the spanwise flow visualization, only the studio light was employed for illumination; images were recorded on a motor-driven Nikon F-3 35 mm camera. A laboratory microcumputer synchronized the motion of the cylinder and the firing of the 35 mm camera using digital control.

The velocity fluctuations in the near-wake region were determined using hot-film anemometry. A Dantec single element R-11 hot-film probe was used in conjunction with a Dantec constant temperature anemometer and a Tektronix differential amplifier. The velocity signals were stored and analysed on the Zenith 241 microcomputer. The usual precautions of signal processing were followed, including analog filtering to prevent aliasing and proper selection of sampling time, relative to the frequencies of interest. The hot-film probe was located at $x/D = 6, y/D = 2$ during measurements. this location was found to be most representative for characterizing the wake response and was compatible with the location of the flow-visualization wire.

3. Overview of wake response

Based on detailed visualization of the flow structure and measurement of the velocity fluctuations, both referenced to the instantaneous displacement of the cylinder, it is possible to define the overall response at a given excitation frequency at the two representative spanwise locations *a* and *b*, illustrated in figure 2. At these midplane *b* and off-midplane *a* locations, it is possible to attain a phase-locked or 'locked-in' response of the vortex formation relative to the instantaneous position of the cylinder. The upper and lower limits of the lock-in regions at the midplane and off-midplane regions cannot occur at the same values of dimensionless excitation frequency f_e/f_0^*, owing to the small difference in cylinder diameter at locations *a* and *b*. The lock-in region at the midplane *b* is translated to a higher-frequency range than that corresponding to the off-midplane *a* location. There is, however, a range of excitation frequencies over which the flow structure is locked-in along the entire span of the cylinder; it is designated as the region of *global lock-in* in figure 2. At the lower boundary of the lock-in region at the midplane *b*, the flow structure transforms into period-doubled vortex formation at $\frac{1}{2}f_0$. A further decrease in excitation frequency produces a more involved modulation of the flow structure. Although the second

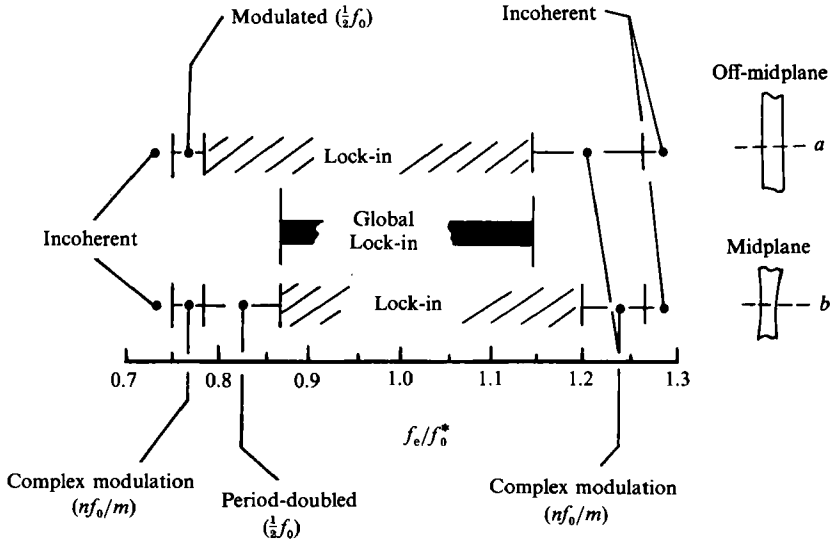

FIGURE 2. Regimes of response of near-wake vortex formation from midplane b region of three-dimensional cylinder and off-midplane a location.

period doubling at $\frac{1}{4}f_0$ was detectable, it was not as consistent as that at $\frac{1}{2}f_0$. A variety of spectral components and their higher-order nonlinear counterparts were evident in the long-time-averaged spectra. We therefore designate this region as complex modulation. Spectral components in this regime were at frequencies nf_0/m, where m and n are integers $1, 2, 3 \ldots$. Corresponding to this region of complex modulation at the midplane b, there occurs modulated vortex formation at the subharmonic $\frac{1}{2}f_0$ at the off-midplane a location. This subharmonic modulation at $\frac{1}{2}f_0$ is not designated as period-doubling since the amplitude of the $\frac{1}{2}f_0$ component does not attain a value commensurate with, or exceeding, that of the fundamental at f_0. Finally, as the excitation frequency is lowered still further, the wake shows an incoherent (or chaotic) response. For excitation frequencies above the regions of lock-in, simple period-doubling was not attainable. Instead, a number of spectral peaks indicative of complex modulation and having values nf_0/m were present. At sufficiently high excitation frequency the wake response becomes incoherent.

Important for our considerations are the following three observations. First, it is possible to attain a globally locked-in response over the entire span of the cylinder, including the three-dimensional non-uniformity, for a given range of excitation frequency f_e/f_0^*. As a consequence, the predominant frequency in the near wake is invariant along the span, but the local phase speed of the vortex formation varies. Secondly, at lower values of excitation frequency ratio f_e/f_0^*, it is possible to maintain a locked-in response in that portion of the wake from the two-dimensional region of the cylinder represented by the off-midplane location a, while localized period-doubling occurs from the three-dimensional portion of the cylinder. Higher-order period-doubling at the midplane, though inconsistent, occurs in the presence of subharmonic modulation at $\frac{1}{2}f_0$ at the off-midplane locations. Thirdly, at large values of excitation frequency ratio f_e/f_0^*, a lock-in condition is maintained in that portion of the wake from the midplane region b, while low-frequency modulations occur in the off-midplane region a. In the following, details association with these phenomena are described using phase-referenced hydrogen-bubble visualization and near-wake velocity measurements.

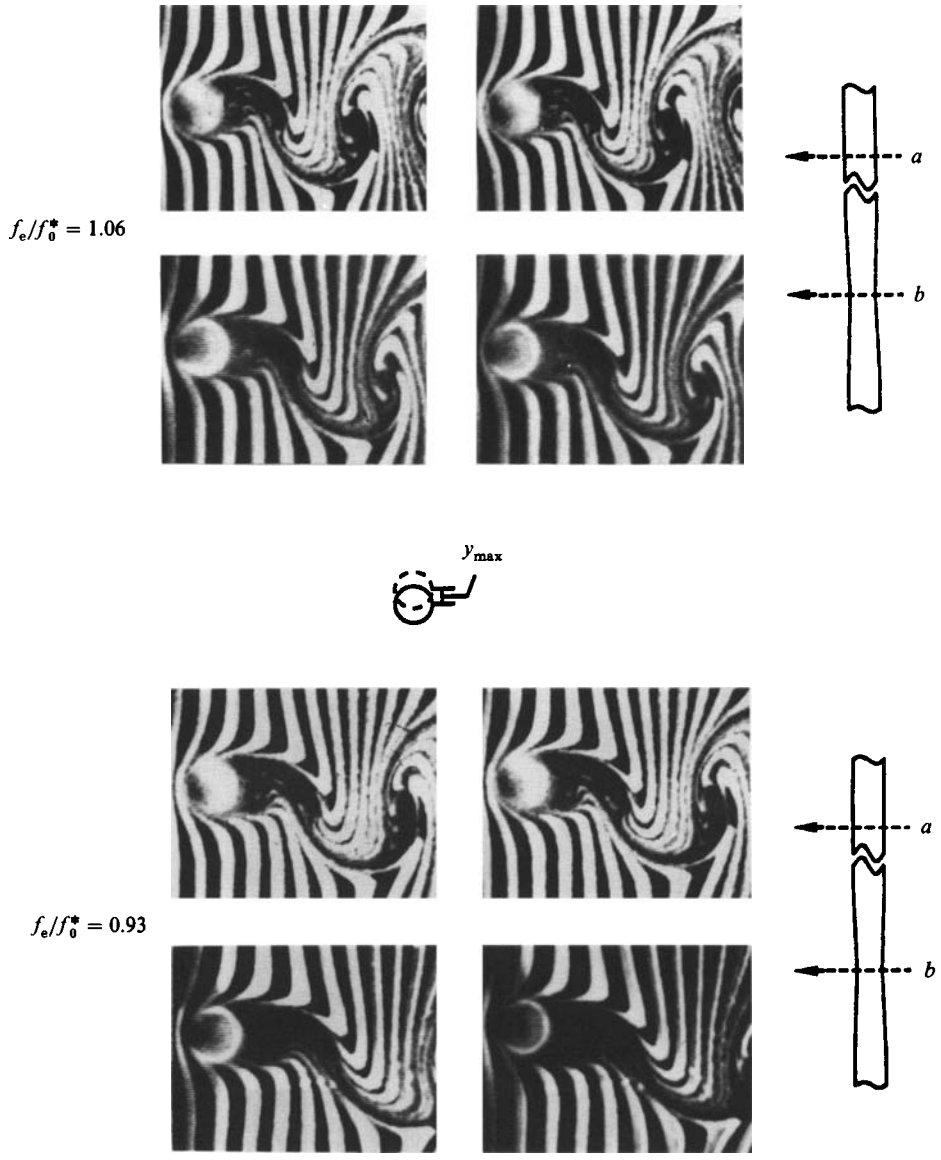

FIGURE 3. Vortex formation visualized in planes orthogonal to cylinder axis at off-midplane a and midplane b locations. All photos taken at instant corresponding to maximum positive displacement of cylinder. Dimensionless excitation frequencies $f_e/f_0^* = 0.93$ and 1.06 correspond to global lock-in of three-dimensional vortex formation along entire span of cylinder.

4. Visualized flow structure in planes orthogonal to cylinder axis

Representative visualization of the flow structure in the global lock-in region is given in figure 3; it corresponds to a frequency ratio $f_e/f_0^* = 1.06$. All photos were taken at an instant corresponding to the maximum positive displacement y_{max} of the cylinder. At both the midplane b and off-midplane a locations, the photos from two successive cylces of oscillation are shown, providing evidence of the locked-in nature of the flow structure. Figure 3 also shows a set of visualization photos within this lock-in region at a lower value of excitation frequency $f_e/f_0^* = 0.93$. At both values of

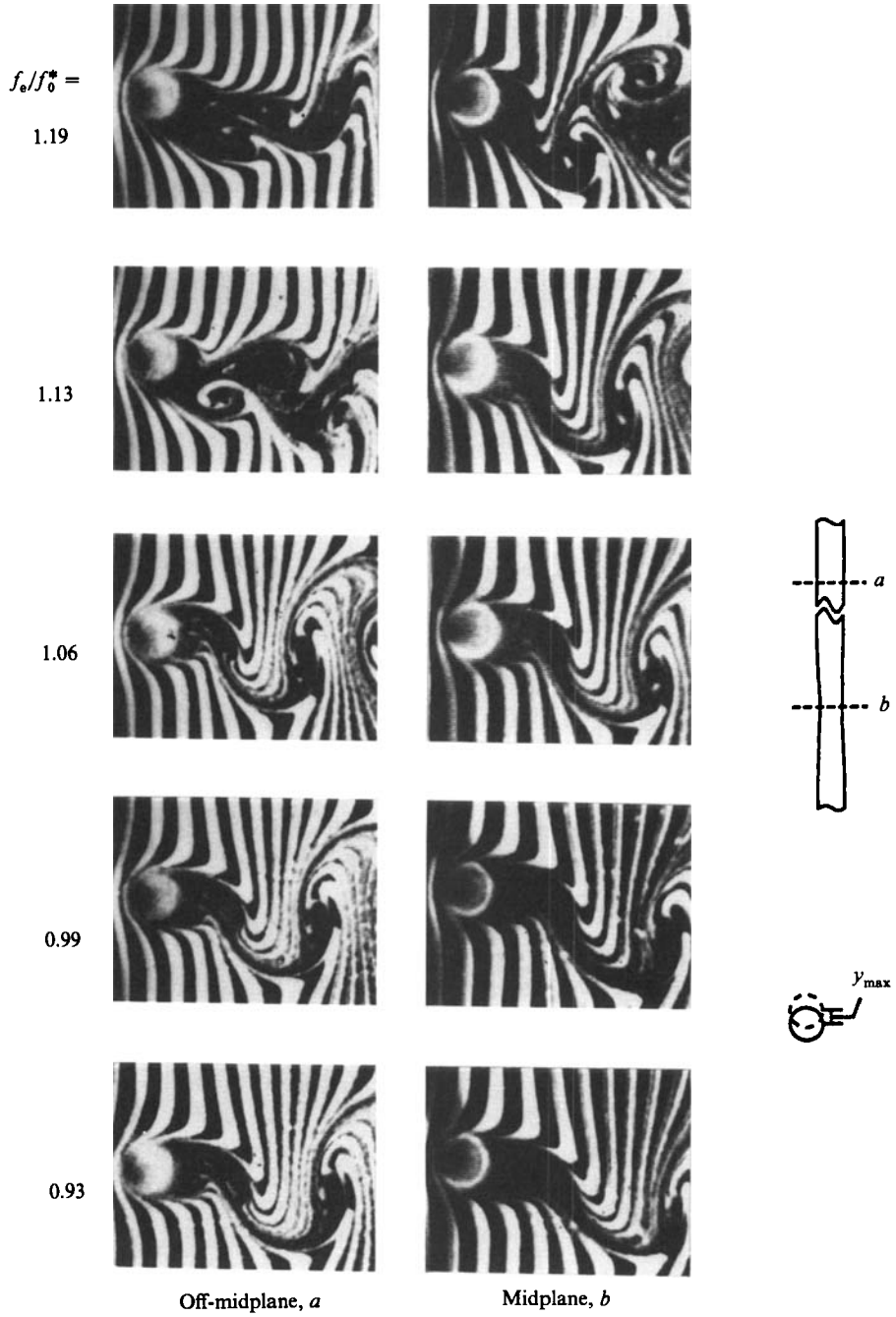

FIGURE 4. Visualization of flow structure in planes orthogonal to axis of cylinder at off-midplane a and midplane b locations. All photos correspond to maximum positive displacement of cylinder. Frequency ratios f_e/f_0^* from 0.93 to 1.13 correspond to global lock-in of vortex formation along entire span of cylinder. At $f_e/f_0^* = 1.19$, vortex formation at midplane b is locked-in, whereas that at off-midplane a location is not.

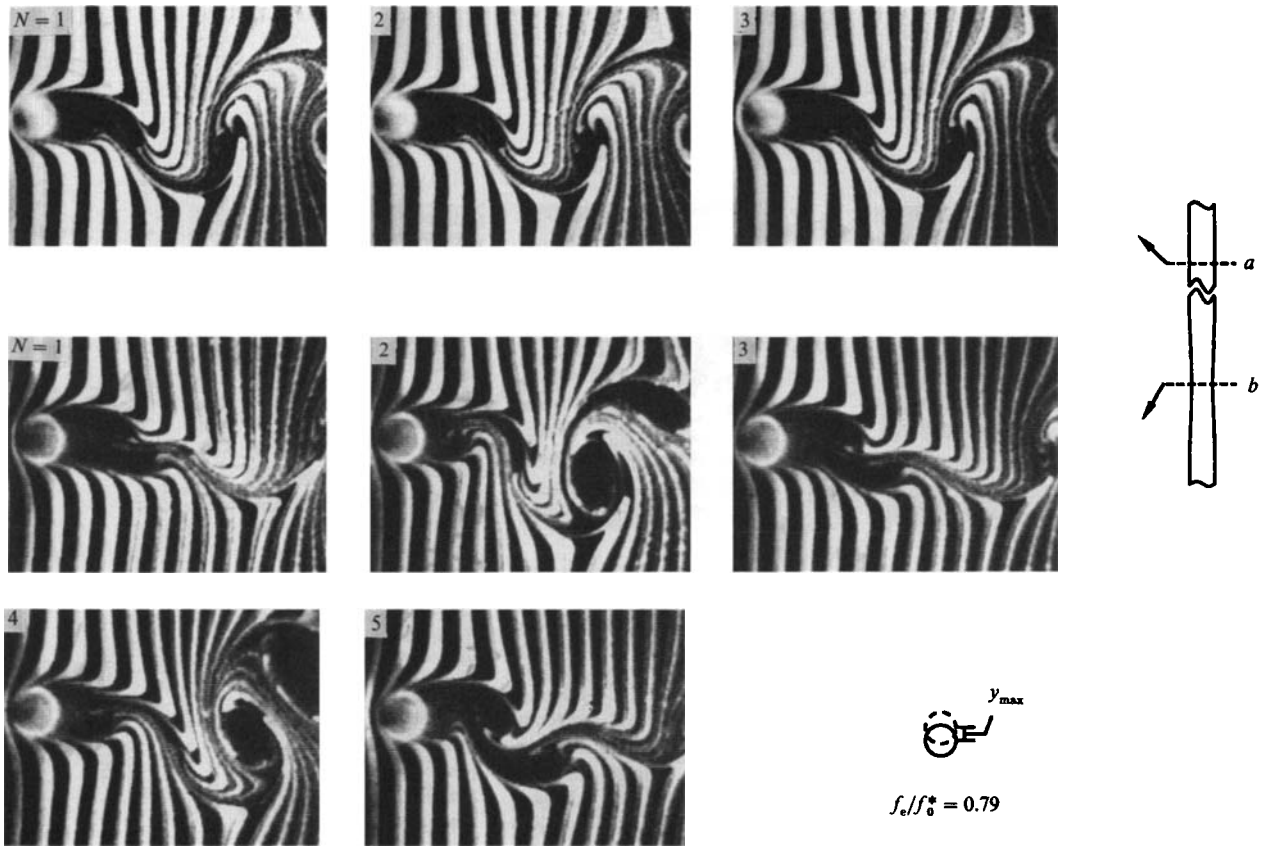

FIGURE 5. Visualization of vortex formation in planes orthogonal to cylinder axis at off-midplane a and midplane b locations. Dimensionless excitation frequency $f_e/f_0^* = 0.79$. All photos correspond to maximum positive displacement of cylinder. At off-midplane a location, vortex formation is locked-in for successive cycles, $N = 1, 2, 3, \ldots$ of cylinder oscillation, while at midplane b location, period-doubled vortex formation occurs and flow pattern is repetitive for every other cycle N of cylinder oscillation.

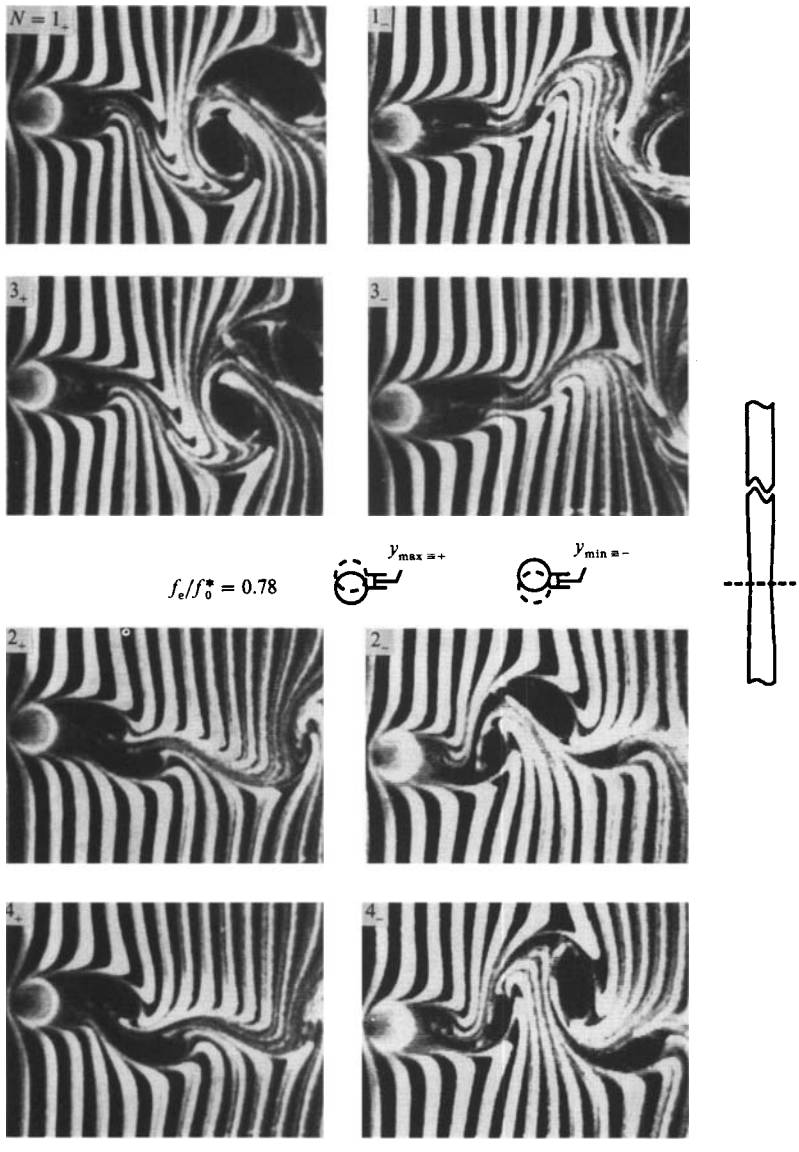

FIGURE 6. Flow visualization of period-doubled vortex formation at midplane of three-dimensional cylinder. Dimensionless excitation frequency $f_e/f_0^* = 0.78$. Photos taken at maximum positive position of cylinder are indicated by plus sign and those at maximum negative position by minus sign, in order to illustrate lack of symmetry of period-doubled vortex formation referenced with respect to cylinder displacement.

frequency ratio shown in figure 3, the vortex pattern at the midplane *b* leads that of the off-midplane *a* location. This lead is apparently due to two effects: a longer formation length and a larger phase speed of the vortices from the midplane. As will be illustrated subsequently, this feature is an essential aspect of the spanwise distortion of the flow structure.

An overview of the effect of frequency ratio f_e/f_0^* on the instantaneous flow structure is given in figure 4. At both the off-midplane and midplane locations *a* and *b*, the initially formed vortex moves downstream with decreasing values of frequency

ratio f_e/f_0^*. At the highest values of frequency f_e/f_0^*, the wake structure collapses to one involving smaller-scale vortices. Nevertheless, it remains phase-locked with respect to the cylinder motion for all cases shown except for the extreme case of $f_e/f_0^* = 1.19$ at the off-midplane location *a*. In this case, the vortex pattern exhibits low-frequency modulations, while that at the midplane *b* remains phase-locked.

Below the lock-in range depicted in figures 3 and 4, the flow structure at the midplane *b* exhibits a well-defined and consistent period-doubling, whereas that in the off-midplane *a* location remains phase-locked, as indicated in the photo layout of figure 5. All photos were taken at the maximum positive displacement y_{max} of the cylinder. Symbol N represents the number of the oscillation cycle. As shown in the top row of photos, at $N = 1$, 2 and 3, the flow structure remains locked-in at the off-midplane location *a*, whereas at the midplane location *b*, it is essentially repetitive only for every other oscillation cycles, namely $N = 1, 3$ and 5, or $N = 2, 4$.

This period-doubled flow structure is not symmetrical with respect to the maximum positive and negative positions of the cylinder, as illustrated in figure 6. The symbols + and − represent respectively the maximum positive and negative positions of the cylinder during an oscillation cycle. The terminology $N = 1_+$ and $N = 1_-$ corresponds to the maximum displacements for the first oscillation cycle. Large-scale vortex formation is particularly evident during odd cycles of the cylinder motion at maximum positive displacement, i.e. $N = 1_+$ and 3_+ and during even cycles at maximum negative displacement, i.e. $N = 2_-$ and 4_-. At the other negative and positive maxima shown in figure 6, i.e. $N = 1_-$ and 3_- and $N = 2_+$ and 4_+. the large-scale vortex formation is initially inhibited.

5. Visualized flow structure along span of cylinder

In order to characterize the three-dimensional structure of the vortex formation in both the lock-in and modulated regimes of response, photos of the spanwise flow structure from the oscillating cylinder were phase-referenced with respect to the cylinder displacement; this technique is analogous to that for the planar visualization described in §4. All photos were taken at an instantaneous cylinder displacement corresponding to the maximum positive position y_{max}, unless otherwise indicated. In all the photos shown in this section, only vortical structures on the near-side of the vortex street are marked.

A representation of the flow structure in the region of lock-in is indicated in figure 7. Two successive cycles of oscillation are shown, in order to emphasize the degree of repeatability. It is evident that the larger formation length and the higher phase speed of the instability from the mid-portion of the cylinder results in larger streamwise displacements of the timelines, relative to the displacements occurring for the two-dimensional regions of the instability at the top and bottom portions of the photo. This observation is in accord with the visualization of figures 3 and 4, which indicates that the vortex formation at the midplane *b* leads that in the two-dimensional, off-midplane *a* location. Comparison of the two photos for cycles $N = 1$ and 2 in figure 7 shows that the structure is phase-locked even in regions downstream as far as $x/D = 24$, corresponding to the right-hand side of each photo. This basic type of flow structure persisted throughout the range of dimensionless excitation frequency f_e/f_0^* corresponding to the global lock-in region defined in figure 2.

The flow structure of the period-doubling process is indicated in figure 8, which shows excerpts from two oscillation cycles of the cylinder. Photos corresponding to $N = 1$ and 2 represent the maximum positive displacement of the cylinder for

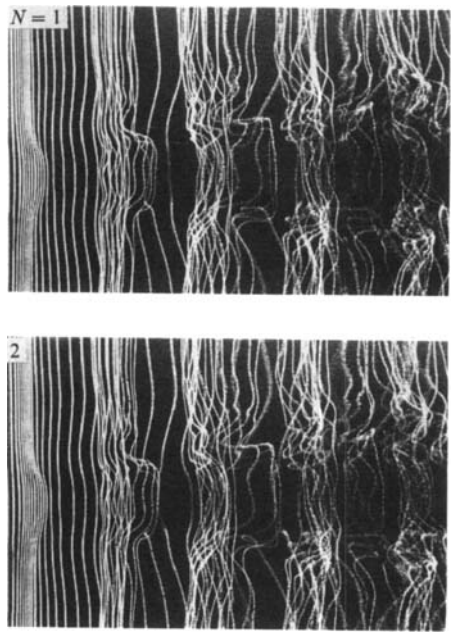

FIGURE 7. Spanwise visualization of global lock-in of vortex formation. Dimensionless excitation frequency $f_e/f_0^* = 0.91$. $N = 1$ and 2 correspond to successive cycles of cylinder oscillation. Vertical and horizontal extents of photograph are $15D$ and $24D$ respectively.

successive cycles of the oscillation. Examination of a large number of phase-referenced photos revealed that those at $N = 1, 3, 5\ldots$ and $N = 2, 4, 6\ldots$ were repeatable, thereby defining a period-doubled oscillation. Fractions of oscillation cycles, indicated by $N = \frac{3}{2}$ and $\frac{5}{2}$, correspond to the maximum negative displacement of the cylinder. The central feature of this period-doubled process is the formation of vortical structures, represented by tightly wound helical roll-ups of the timelines, at angles of the order of 45° with respect to the free stream; taken together, these inclined helical roll-ups form a diamond-shaped pattern. This pattern first appears as the left most vortical structure in the photo taken at $N = \frac{5}{2}$. Its subsequent development in the downstream direction is shown in photos corresponding to $N = 1, \frac{3}{2}$, and 2. Comparing the photos at $N = \frac{3}{2}$ and $\frac{5}{2}$, in particular the left most vortex in each of these photos, it is apparent that the vortex at $N = \frac{3}{2}$ is relatively intact and quasi-two-dimensional, while that at $N = \frac{5}{2}$ 'splits' at its midportion to accommodate the formation of the inclined vortical structures. In a simplified sense, one may therefore view the period-doubled process as the alternating formation of 'unsplit' and 'split' vortices.

In contrast to the present case of an induced period-doubled or subharmonic response in the presence of cylinder forcing at a frequency unrelated to the subharmonic component, Lasheras & Meiburg (1990) considered the case of subharmonic forcing of the wake from a thin flat plate. In their numerical simulation, certain features of the distortion of vortex filaments resemble the timeline patterns of figure 8. In particular, the alternate appearance of so-called split vortical structures and relatively undistorted ones is suggested in their investigation. The period-doubled response of figure 8 appears, on the other hand, to be distinct from the chevron-shaped patterns of oblique vortices, characterized by Williamson (1989).

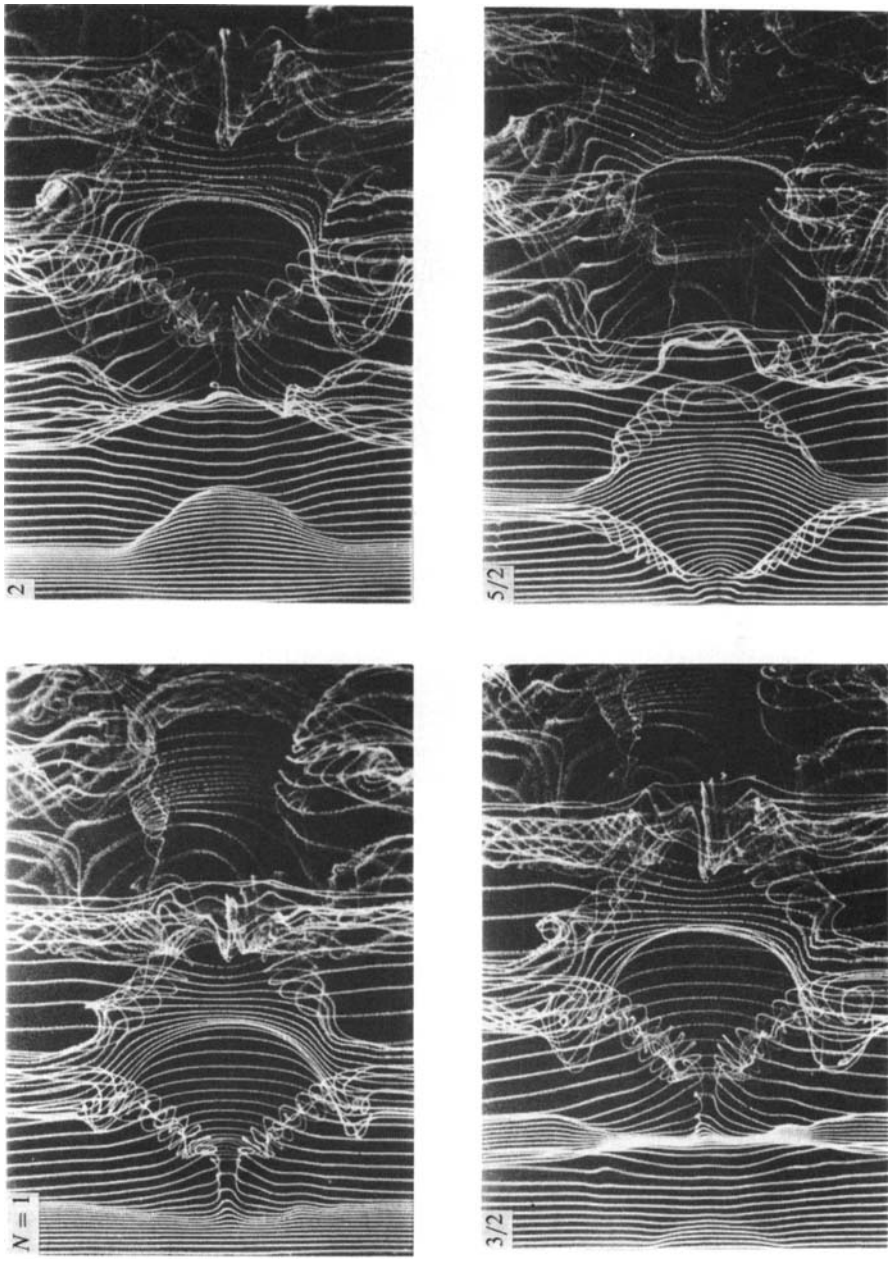

FIGURE 8. Spanwise visualization of period-doubled vortex formation. Photos designated as $N = 1$ and 2 correspond to maximum positive displacement of cylinder for two successive cycles of oscillation. Photos $N = 3/2$ and 5/2 are taken at maximum negative displacement. Vertical and horizontal extents of each photograph are $15D$ and $24D$ respectively. Dimensionless excitation frequency is $f_e/f_0^* = 0.81$.

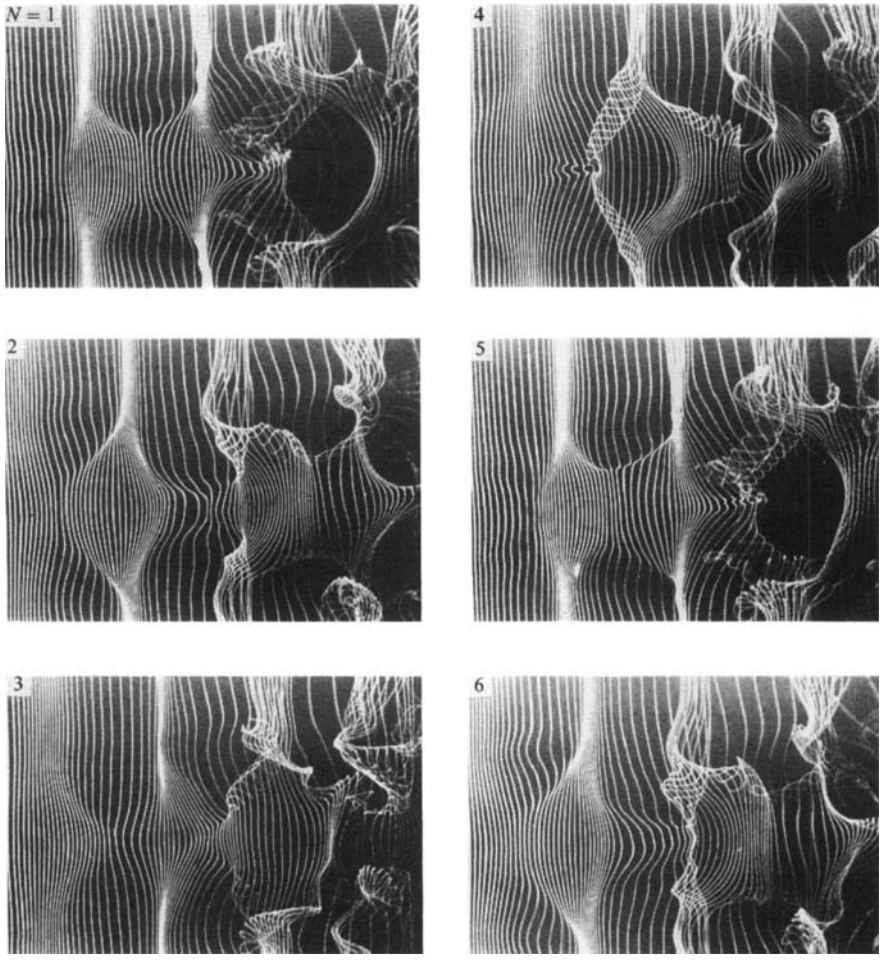

FIGURE 9. Spanwise visualization of second period-doubling. Photos designated as $N = 1$ through 6 all taken at maximum instantaneous displacement of cylinder over six successive cycles. Dimensionless excitation frequency is $f_e/f_0^* = 0.78$. Vertical and horizontal extents of each photograph are $15D$ and $24D$ respectively.

This oblique vortex formation is strongly influenced by the end conditions of the stationary cylinder; no period-doubling or subharmonic generation is suggested by the dye visualization patterns of that investigation.

If the excitation frequency is lowered still further, then just prior to the onset of incoherent (chaotic) motion, the next period-doubling can be observed. This case, corresponding to repetition of the flow structure every four cycles of the cylinder oscillation, is indicated in figure 9. Each photo therein is taken at the maximum positive displacement of the cylinder. A central feature of this higher-order period-doubled process is again the occurrence of 'split' vortices evident, for example, at the right of photo $N = 1$, at the left of photo $N = 2$, and near the middle of photo $N = 4$. The splitting of vortices can apparently occur in several fashions and is interspersed among complex types of vortex development. Despite this complexity, however, the photos corresponding to $N = 1, 5$ and $N = 2, 6$ show remarkably repeatable flow structure, even in the furthest downstream region.

From the foregoing, it is evident that certain three-dimensional features of the

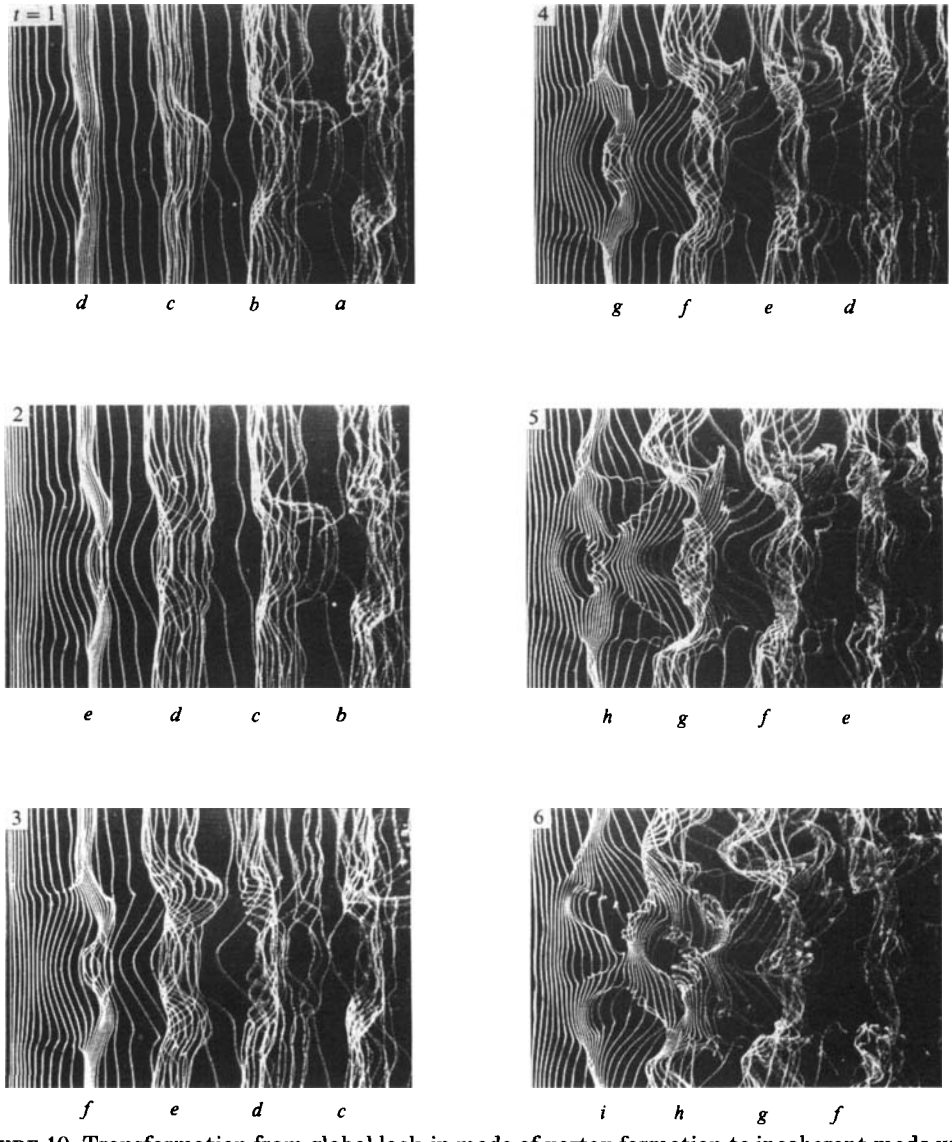

FIGURE 10. Transformation from global lock-in mode of vortex formation to incoherent mode upon abrupt cessation of cylinder motion at $t = 0$. Times $t = 1$–6 correspond to instant of appearance of second vortex from left of each photo. Excitation frequency is $f_e/f_0^* = 0.97$ upon cessation of motion. Vertical and horizontal extents of each photograph are $15D$ and $24D$ repectively.

timeline patterns are generic to each of the successive period-doublings. The question arises as to whether these features, including vortex splitting, emerge from an inherent three-dimensional instability when the flow pattern undergoes transient transformation from a locked-in to an incoherent state. In order to investigate such a possibility, the cylinder was oscillated at an excitation frequency corresponding to lock-in, in order to attain repetitive flow structure from cycle to cycle. Then, the motion of the cylinder was abruptly stopped and the evolution of the three-dimensional flow pattern was observed. Figure 10 shows the transformation of the flow structure during this process. Photographs corresponding to $t = 1, 2, \ldots, 6$ are phase-referenced with respect to the appearance of the second vortical structure from

the left-hand side of each photo. At $t = 1$, it corresponds to vortex c, at $t = 2$ to vortex d, etc. At this spatial location, the spanwise structure of the vortex becomes increasingly three-dimensional and finally, at $t = 5$, an apparent vortex splitting occurs. It initiates with splitting of the left most vortex g at $t = 4$. Its successor, vortex h at $t = 5$, also undergoes a similar process of splitting. Such successive splitting cannot be maintained indefinitely, however, and as shown at time $t = 6$ in figure 10, the three-dimensional flow structure has progressed well towards an incoherent state.

6. Velocity fluctuations in the near wake

The states of response of the wake, defined in the overview of figure 2 and the visualization in the preceding sections, were further characterized by measurement of the near-wake velocity fluctuations. Traces of velocity versus time, for excitation conditions ranging from the lock-in state to the onset of incoherent motion, are illustrated in figures 11–14. The case of global lock-in, whereby the flow structure along the entire span is phase-locked with respect to the motion of the cylinder, is represented by the two traces in the left column of figure 11. The lower trace was taken at the midplane b and the upper at the off-midplane a location. This global lock-in generates a velocity trace $u(t)$ that is nearly sinusoidal, with no detectable modulations.

The period-doubled response of the wake is represented by the lower velocity trace in the middle column of figure 11. The upper trace indicates that the vortex formation in that portion of the wake is still highly periodic with insignificant modulation, and thereby locked-in. The drastic differences between these traces in the middle column of figure 11 emphasizes the fact that the period-doubled wake instability from the three-dimensional portion of the cylinder is indeed a localized phenomenon.

A more complex modulation of the wake structure is shown in the traces of the right-hand column of figure 11. Instead of the simple period-doubled response of the central portion of the wake from the three-dimensional region of the cylinder evident at the higher value of excitation frequency, there appears a more complex modulation. Even though the larger-amplitude positive peaks appear to repeat approximately every fourth period of the primary oscillation, suggesting occurrence of the second period-doubling, this pattern was not consistent in the long-time sense. In the off-midplane region, represented by the top trace, there is a distinct subharmonic modulation at $\frac{1}{2}f_0$. This modulation, however, does not give way to fully-developed period-doubling before it collapses to an incoherent state. We conclude, on the basis of the traces of figure 11, that the loss of a well-defined, period-doubled wake from the three-dimensional portion of the cylinder is accompanied by onset of subharmonic modulation in the flow structure exterior to this region.

7. Spectra of near-wake velocity fluctuations

Spectra of the near-wake velocity fluctuations characteristic of the lock-in state are illustrated in figure 12. The predominant peak of the near-wake instability, i.e. the vortex formation, occurs at the same frequency for the midplane b and off-midplane a locations, emphasizing the occurrence of the global lock-in along the entire span of the cylinder.

The spectrum at the top of the left-hand column of figure 12 shows the case of lock-

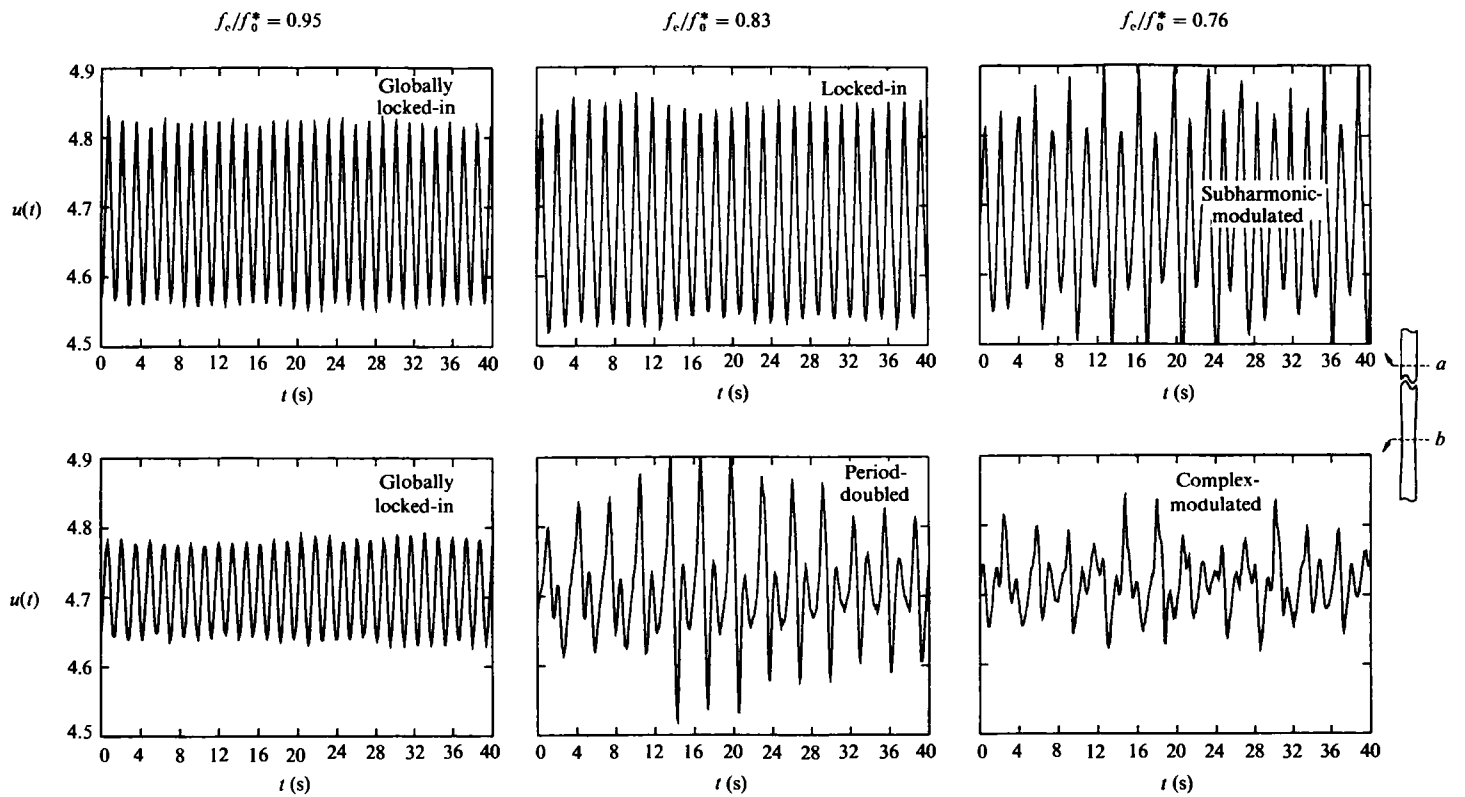

FIGURE 11. Velocity traces taken in near-wake at spanwise locations corresponding to off-midplane a and midplane b for basic states of response: (a) global lock-in along entire span of cylinder at $f_e/f_0^* = 0.95$; (b) localized period-doubling from three-dimensional region of cylinder embedded within locked-in vortex formation at $f_e/f_0^* = 0.83$; and (c) complex modulation of three-dimensional vortex formation embedded within subharmonic-modulated vortex formation at $f_e/f_0^* = 0.76$.

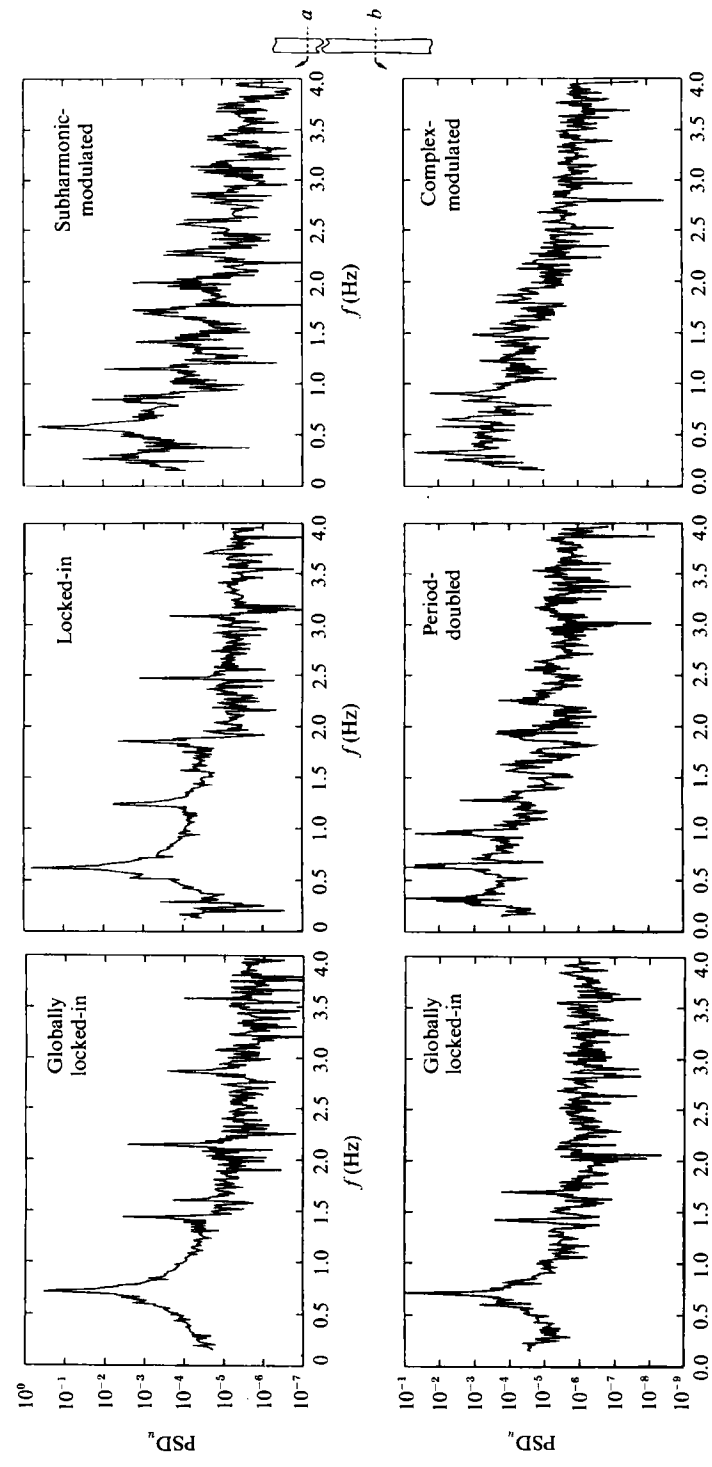

FIGURE 12. Power spectral density of velocity fluctuation in wake for basic states of response (*a*) global lock-in along entire span of cylinder at $f_e/f_0^* = 0.95$; (*b*) period-doubled three-dimensional vortex formation embedded within two-dimensional vortex formation at $f_e/f_0^* = 0.83$; and (*c*) complex modulation embedded within subharmonic modulated vortex formation at $f_e/f_0^* = 0.76$.

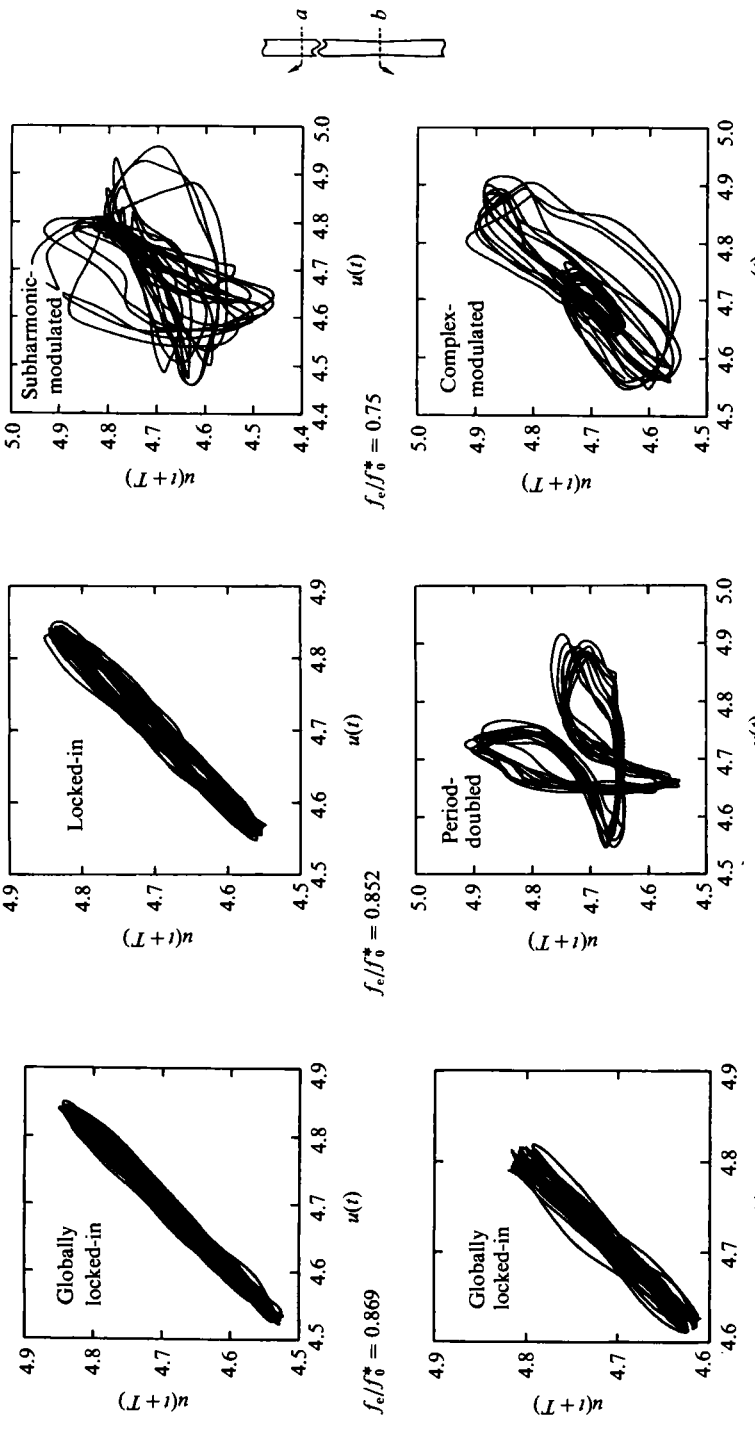

FIGURE 13. Phase plane portraits constructed from velocity measurements for (*a*) global lock-in along entire span of cylinder at threshold of period-doubling at $f_e/f_0^* = 0.869$; (*b*) period-doubled three-dimensional vortex formation from midplane *b* embedded within locked-in vortex formation represented by off-midplane location *a* at $f_e/f_0^* = 0.852$; and (*c*) onset of incoherent vortex formation at $f_e/f_0^* = 0.75$ characterized by region of complex modulation at midplane *b* and subharmonic modulation at off-midplane *a* location.

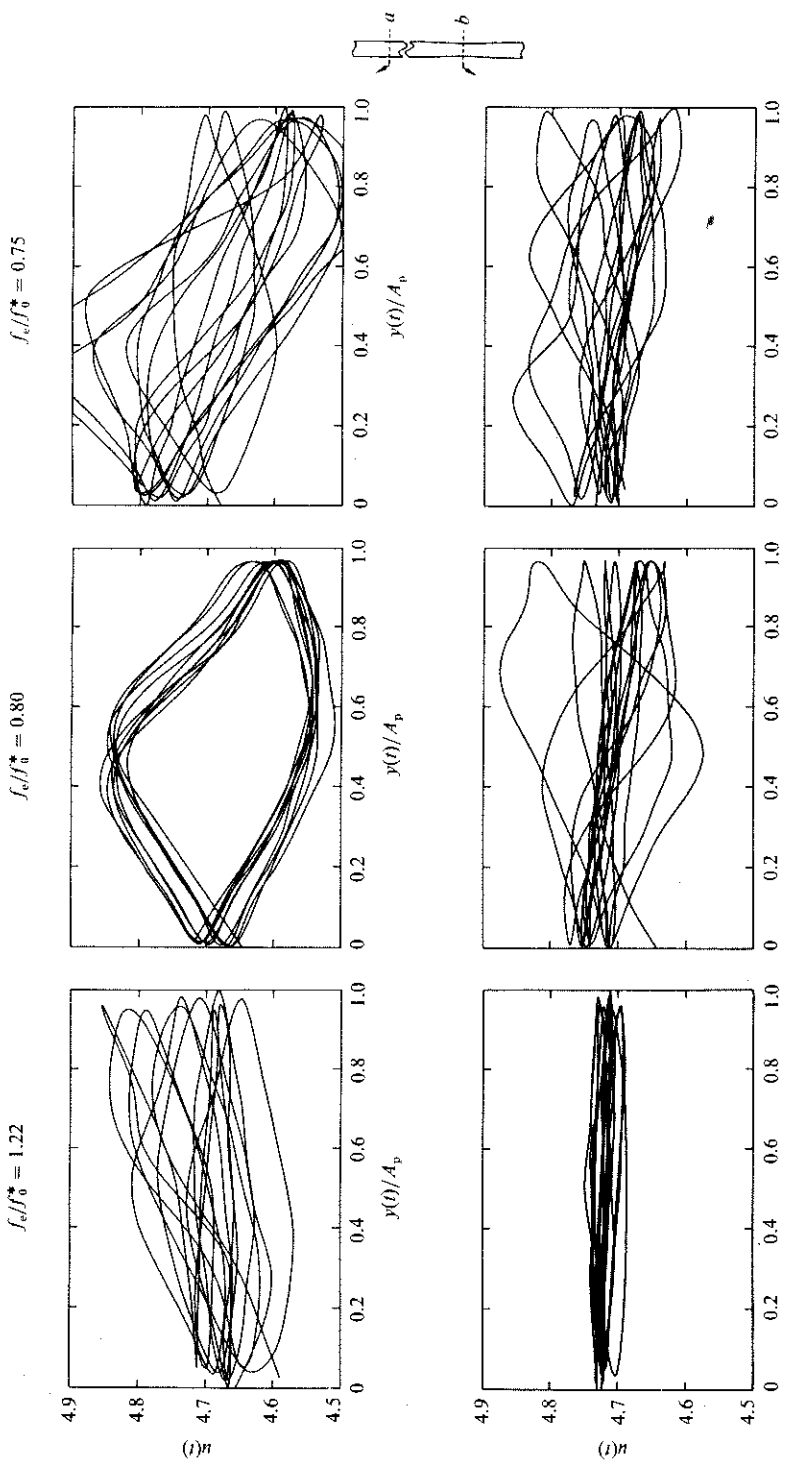

FIGURE 14. Phase plane plots showing degree of phase coherence between near-wake velocity fluctuation $u(t)$ and cylinder displacement $y(t)$, normalized by peak to peak amplitude A_p for dimensionless excitation frequencies $f_e/f_0^* = 1.22$, 0.80 and 0.75 (from left to right).

in response of the wake at the off-midplane a location. Correspondingly, at the midplane b location, there appears the period-doubled component $\frac{1}{2}f_0$ and the higher-order components at $f_0, f_0+\frac{1}{2}f_0$, and so on.

Increased irregularity of the spectrum at the midplane b location is evident in the bottom spectrum in the right-hand column of figure 12, corresponding to the regime of complex modulation defined in figure 2. It is characterized by a number of discrete, nonlinearly interacting spectral components. Correspondingly, at the off-plane a location, illustrated by the top spectrum in the right-hand column of figure 12, the existence of the fundamental f_0, its subharmonic $\frac{1}{2}f_0$, and higher-order components due to nonlinear interaction are all apparent.

8. Phase plane representations

Phase plane representations of the near-wake velocity are given in figure 13. These phase planes are plotted in terms of $u(t+T)$ *vs.* $u(t)$, where T is the time delay; it corresponds to the reciprocal of the frequency of the predominant peak in the velocity spectra. Ten successive, but randomly selected, cycles of oscillation are shown for illustration in these phase plane plots. This approach allows clear interpretation of, and comparison with, the phase plane representations of the incoherent (chaotic) fluctuations of velocity u. In the following, we describe phase planes at selected excitation frequencies f_e/f_0^*, in order to show the transformation from the case where the vortex formation is essentially locked-in along the entire span of the cylinder, to the onset of incoherent (chaotic) response of the wake.

The phase planes in the left-hand column of figure 13 correspond to the locked-in region of vortex formation, where the predominant spectral component occurs at the vortex formation frequency f_0. Corresponding spectra (not shown) of velocity u show a negligible amplitude of the subharmonic $\frac{1}{2}f_0$ at the off-midplane a location; at the midplane b location, however, this component $\frac{1}{2}f_0$ was significant, marking the very initial stage of the period-doubling process. For this reason, the phase plane plot at the midplane b location shows more jitter than the off-midplane location. It is evident that the average slopes of the traces at both off-midplane a and midplane b locations are the same, suggesting the same apparent phase angle of the velocity fluctuation along the entire span of the cylinder.

In the phase planes of the middle column of figure 13, the process of period-doubling has been attained at the midplane b location, while the lock-in state at the fundamental f_0 persists in the off-midplane region a, i.e. over the entire region exterior to the three-dimensional portion of the cylinder.

The plots in the right-hand column of figure 13 suggest a high degree of disorganization at both midplane b and off-midplane a locations. This lack of organized response is associated with a substantial number of ill-defined peaks in the spectra (not shown) at both the midplane b and the off-midplane a locations.

In order to represent the phase coherence between the downstream development of the three-dimensional vortical structures and the forced motion of the cylinder, the velocity fluctuation $u(t)$ was recorded simultaneously with the instantaneous displacement $y(t)$ of the cylinder, leading to phase plane representations $u(t)$ *vs.* $y(t)$. The peak to peak amplitude A_p of the cylinder is used for normalization. Here we focus on the degree of phase coherence between $u(t)$ and $y(t)$ at relatively high and low frequencies. The intent is to emphasize the switch in the phase coherence between the midplane b and the off-midplane a portions of the cylinder at the extreme values of forcing frequency f_e/f_0^*.

At the largest value of excitation frequency $f_e/f_0^* = 1.22$ shown in the left-hand column of figure 14, we see a high degree of phase coherence between the cylinder motion and the near-wake response at the midplane location b. On the other hand, it is evident that at the off-midplane location a, there is substantial phase drift between $u(t)$ and $y(t)$ from cycle to cycle of the cylinder motion. In essence, the phase planes in the left column illustrate the phase-coherent nature of the flow structure from the midplane b, i.e. the three-dimensional portion of the cylinder, and the lack of phase-coherent response exterior to this region. These phase plane plots compare with the flow visualization at the highest excitation frequency $f_e/f_0^* = 1.19$ in figure 4. Therein, it is shown that existence of a highly organized, small-scale vortex street from the midplane b of the cylinder allows a phase-locked response of the vortex pattern. On the other hand, at the off-midplane location, this type of phase-locked pattern is not attainable.

The converse of this situation is illustrated in the phase plane at the top of the middle column of figure 14. The flow structure from the off-midplane location a, i.e. exterior to the three-dimensional region of the cylinder, is phase-locked to the cylinder motion. On the other hand, there is less coherence of the period-doubled response at the midplane location b.

Viewing together the phase plane plots in the left-hand and middle columns of figure 14, we conclude that it is possible to have a localized region of phase coherent response between the cylinder motion and the near-wake instability bounded by a region(s) of phase-incoherent response. The spanwise location at which the region of coherent phase response exists can be switched by changing the dimensionless forcing frequency.

Finally, figure 14(c) shows the case where the traces $u(t)$ *vs.* $y(t)$ are phase incoherent (chaotic) along the entire span of the cylinder.

9. Concluding remarks

Lock-in (phase-locking) of the near-wake vortex formation can be attained along the entire span of the three-dimensional cylinder over a reasonably wide range of excitation frequency. Such global lock-in means that the three-dimensional vortex patterns are repetitive from cycle to cycle of the cylinder motion. When this lock-in occurs, the frequency of formation of the three-dimensional vortices is constant along the span of the flow. However, the phase speed of the localized vortex formation from the three-dimensional region of the cylinder exceeds that from the two-dimensional region, thereby generating a three-dimensional pattern of vortex formation that remains phase-locked. The fact that a locked-in state can exist along the entire span of the non-uniform cylinder has important implications for self-excited vibrations of structural configurations having non-uniformities. Existence of a locked-in state provides the potential for self-excited vibration of the corresponding elastic or elastically-mounted structure.

At the lower boundary of the lock-in region, the flow structure from the three-dimensional portion of the cylinder exhibits a period-doubled response. This structure is embedded within regions of two-dimensional, phase-locked vortex formation on either side of it. In other words, there occurs a localized region of period-doubling bounded on either side by regions of locked-in vortex formation. The mechanism of this period-doubled vortex formation involves formation of 'split' vortices during every other cycle of the cylinder motion. This pattern of period-doubled vortex formation contrasts sharply with that corresponding to the case where locked-in

vortex formation occurs along the entire span of the flow. Such period-doubling is distinctly different from the well-known subharmonic generation occurring in free shear layers, where merging or coalescence of the adjacent vortices gives rise to a pronounced subharmonic component (Ho & Huerre 1984). In the present study, the occurrence of alternate states of split and unsplit vortices characterizes the period-doubling process. This type of period-doubling is related to that found numerically for the case of instabilities from a cylinder having spanwise uniformity, but non-uniform flow structure (Karniadakis & Triantafyllou 1990). In their observations, vortex coalescence did not occur, yet pronounced subharmonic components were generated.

A second period-doubling of the wake from the three-dimensional portion of the cylinder could be captured by flow visualization; however it was not consistent in the long-time sense. In this state of the wake response, the vortex shedding from the two-dimensional portion of the cylinder is modulated at the subharmonic of the natural shedding frequency. This region of vortex formation normally exhibits a locked-in response when there is simple period-doubling of the three-dimensional vortex formation from the mid-portion of the cylinder. It is possible that the competition between the modulated response of the vortex formation from the two- and three-dimensional portions of the cylinder inhibits higher-order period-doubling of the shedding process. In fact, intermittent oscillations at one-third the fundamental were observed from time to time. It should be noted that additional period-doublings beyond the first one were not attainable in analogous open-flow experiments involving instabilities through a cantilevered pipe investigated by Paidoussis & Moon (1988). Moreover, they observed one-third and two-thirds subharmonic modulations, and rarely a one-fourth modulation, after the first period-doubling.

Whereas all of the foregoing observations of period-doubling and subharmonic modulation occur at the lower end of the lock-in region, excitation at successively higher frequencies at the upper end of the lock-in region did not produce simple period-doubling; rather, more complex modulation patterns were observed. They were associated with the generation of spectral components corresponding to various subharmonics of the natural shedding frequency. An important observation, however, is the attainment of a locked-in, or phase-locked, response of the flow structure from the three-dimensional portion of the cylinder, while that in the regions on either side of it, i.e. from the two-dimensional portions, is modulated. In other words, the scenario is the converse of that occurring for excitation at the lower end of the locked-in region where the aperiodic response first occurs from the three-dimensional portion of the cylinder.

The authors gratefully acknowledge financial support of the Office of Naval Research and the National Science Foundation.

REFERENCES

Chomaz, J. M., Huerre, P. & Redekopp, L. T. 1988 Bifurcations to local and global modes in spatially developing flows. *Phys. Rev. Lett.* **60**, 25–28.

Feigenbaum, M. J. 1980 The transition to aperiodic behavior in turbulent systems. *Commun. Math. Phys.* **77**, 65–86.

Gerrard, J. H. 1978 The wakes of cylindrical bluff bodies at low Reynolds number. *Proc. R. Soc. Lond.* A **288**, 351–382.

Giglio, M., Musazzi, S. & Perini, U. 1981 Transition to chaotic behavior viz. a reproducible sequence of period-doubling bifurcations. *Phys. Rev. Lett.* **47**, 243–246.

Gollub, J. P. & Benson, S. V. 1980 Many routes to turbulent convection. *J. Fluid Mech.* **100**, 449–470.

GOLLUB, J. P., BENSON, S. V. & STEINMAN, J. 1980 A subharmonic route to turbulent convection. *Ann. N.Y. Acad. Sci.* **357**, 22–27.

HO, C.-M. & HUERRE, P. 1984 Perturbed free shear layers. *Ann. Rev. Fluid Mech.* **16**, 365–424.

HUERRE, P. & MONKEWITZ, P. A. 1985 Absolute and convective instabilities in free shear layers. *J. Fluid Mech.* **159**, 151–168.

KARNIADAKIS, G. E. & TRIANTAFYLLOU, G. S. 1989*a* Frequency selection and asymptotic states in laminar wake. *J Fluid Mech.* **199**, 441–469.

KARNIADAKIS, G. E. & TRIANTAFYLLOU, G. S. 1989*b* The crisis of transport measures in chaotic flow past a cylinder. *Phys. Fluids* A **1**, 628–630.

KARNIADAKIS, G. E. & TRIANTAFYLLOU, G. S. 1990 Period doubling cascade in the wake of a circular cylinder. *Bull. Am. Phys. Soc.* **35**, 2242.

KARNIADAKIS, G. E. & TRIANTAFYLLOU, G. S. 1992 Three-dimensional dynamics and transition to turbulence in the wake of bluff objects. *J. Fluid Mech.* **238**, 1–30.

KOCH, W. 1985 Local instability characteristics and frequency determination of self-excited wake flows. *J. Sound Vib.* **99**, 53–83.

LASHERAS, J. C. & MEIBURG, E. 1990 Three-dimensional vorticity modes in the wake of a flat plate. *Phys. Fluids* A **2**, 371–379.

MEIBURG, E. & LASHERAS, J. C. 1988 Experimental and numerical investigation of the three-dimensional transition in plane wakes. *J. Fluid Mech.* **190**, 1–37.

MONKEWITZ, P. A. 1988 The absolute and convective nature of instability in two-dimensional wakes at low Reynolds number. *Phys. Fluids* **31**, 999–1006.

MONKEWITZ, P. A. & NGUYEN, L. N. 1987 Absolute instability in the near-wake of three-dimensional bluff bodies. *J. Fluids Struct.* **1**, 165–184.

OLINGER, D. J. & SREENIVASAN, K. R. 1988 Nonlinear dynamics of the wake of an oscillating cylinder. *Phys. Rev. Lett.* **60**, 797–800.

ONGOREN, A. & ROCKWELL, D. 1988*a* Flow structure from an oscillating cylinder. Part 1. Mechanisms of phase shift and recovery of the near wake. *J. Fluid Mech.* **191**, 197–223.

ONGOREN, A. & ROCKWELL, D. 1988*b* Flow structure from an oscillating cylinder. Part 2. Load competition in the near wake. *J. Fluid Mech.* **191**, 225–245.

PAIDOUSSIS, M. E. & MOON, F. C. 1988 Nonlinear and chaotic fluid elastic vibrations of a flexible pipe conveying fluid. *J. Fluids Struct.* **2**, 567–591.

ROCKWELL, D., MAGNESS, C. & NUZZI, F. 1990 The locked-in and period-doubled wake from a nonuniform cylinder. *Bull. Am. Phys. Soc.* **35**, 2252.

ROCKWELL, D., NUZZI, F. & MAGNESS, C. 1991 Period doubling in the wake of a three-dimensional cylinder. Letter to Editor. *Phys. Fluids* A **3**, 1477–1478.

SREENIVASAN, K. R. 1985 Transition and turbulence in fluid flows and low-dimensional chaos. In *Frontiers in Fluid Mechanics* (ed. S. H. Davis & J. L. Lumley), pp. 41–67. Springer.

TRIANTAFYLLOU, G. S. 1990 Three-dimensional flow patterns in two-dimensional wakes. *ASME Symp. on Unsteady Flows, Joint Meeting of ASME and CSME, June 4–10, University of Toronto, Toronto, Canada*, pp. 395–402.

TRIANTAFYLLOU, G. S., TRIANTAFYLLOU, M. S. & CHRYSSOSTOMODIS, C. 1986 On the formation of vortex streets behind circular cylinders. *J. Fluid Mech.* **170**, 461–477.

UNAL, M. F. & ROCKWELL, D. 1988 Vortex formation from a cylinder. Part 1. The initial instability. *J. Fluid Mech.* **190**, 491–512.

VAN ATTA, C. W. & GHARIB, M. 1987 Ordered and chaotic vortex streets behind circular cylinders at low Reynolds numbers. *J. Fluid Mech.* **174**, 113–133.

WILLIAMSON, C. & ROSHKO, A. 1988 Vortex formation in the wake of an oscillating cylinder. *J. Fluids Struct.* **2**, 355–381.

WILLIAMSON, C. H. K. 1989 Oblique and parallel modes of vortex shedding in the wake of a circular cylinder at low Reynolds numbers. *J. Fluid Mech.* **206**, 579–627.